Bursting oscillation in CO oxidation with small excitation and the enveloping slow-fast analysis method*

Li Xiang-Hong(李向红)[a)b)] and Bi Qin-Sheng(毕勤胜)[a)†]

[a)] *Faculty of Civil Engineering and Mechanics, Jiangsu University, Zhenjiang* 212013, *China*
[b)] *Department of Mathematics and Physics, Shijiazhuang Tiedao University, Shijiazhuang* 050043, *China*

(Received 22 February 2012; revised manuscript received 5 March 2012)

Based on the traditional scheme for a nonlinear system with multiple time scales, the enveloping slow-fast analysis method is developed in the paper, which can be employed to investigate the dynamics of nonlinear fields with multiple time scales with periodic excitation. Upon using the method, the behaviors of the kinetic model of CO oxidation on the platinum group metals have been explored in detail. Two typical bursting phenomena such as Fold/Fold/Hopf bursting and Fold/Fold bursting, are presented, the bifurcation mechanisms of which have been obtained. Furthermore, the dynamic difference between the two cases corresponding to relatively large and small perturbation frequencies, respectively, has been presented, which can be used to describe the influence of the frequencies involving in the evolution on the bursting behaviors in the system.

Keywords: CO oxidation, bursting phenomenon, bifurcation mechanism, enveloping slow-fast analysis

PACS: 05.45.–a, 82.40.Bj **DOI:** 10.1088/1674-1056/21/6/060505

1. Introduction

Many chemical systems refer to multiple time scales, since an order gap may exist between the rates associated with different steps of chemical reactions, in which some special phenomena such as steady-state multiplicity, relaxation oscillations, and chaos can be observed.[1,2] The dynamics of the chemical systems often behave in periodic oscillation with large-amplitude oscillations characterized by small-amplitude oscillations, which can be called a bursting oscillation.[3] Many studies have reported the investigation of the mechanism of the relaxation or the complex irregular oscillation.[4,6] However, up to now, only a few results related to some simple reaction oscillations have been published,[6] while for a general chemical reaction, it is still an open problem, especially when time-dependent perturbation is involved.

In this paper, we focus on the heterogeneous catalytic reactions of the CO oxidation on the platinum group metals, which is one of the most widely studied reactions related to multiple time scales.[7] There have been many efforts to explain theoretically the relaxation oscillations with different hypotheses, such as the dependence of activation energy on the surface coverage, the formation of the metal oxide, and the absorbate induced reversible surface transformation.[8−10] Based on the experimental observation, some oxygen atoms can penetrate into the subsurface layers to cause both structural and chemical modification of the adsorption sites, which may lead to different reaction rates with order gap in the whole kinetic model, resulting in the system with multiple time scales, on the facts that the processes of formation of the subsurface oxygen and its interaction with the adsorbed CO are slower than the adsorption, desorption, and interaction of adsorbed species.[11−13]

Here we consider dynamics of the kinetic model with small periodic perturbation, which occurs on the dimensionless concentration of CO absorbed on the surface. Though the bifurcation mechanisms of a few models, such as the neuronal system,[14] the controlled Lorenz oscillator,[15] CO oxidation,[16] and the B–Z reaction,[17] have been obtained in previous papers. However, for a system with periodic perturbation, slow–fast analysis cannot be directly used to explore the mechanism of the bursting behavior of the system.[18] In this paper, we develop a new method, called enveloping slow–fast analysis, to investigate the dynamical behavior of the model. Some

*Project supported by the National Natural Science Foundation of China (Grant Nos. 20976075, 20976041, and 10972091).
†Corresponding author. E-mail: qbi@ujs.edu.cn
© 2012 Chinese Physical Society and IOP Publishing Ltd

relaxation oscillations such as Fold/Fold/Hopf bursting and Fold/Fold bursting have been observed, and the bifurcation mechanisms are obtained to account for the corresponding phenomena. Furthermore, the influence of the parameters on the dynamics of the system is presented.

2. Mathematical model

Consider the kinetic scheme of CO oxidation on the platinum group metals based on the Langmuir–Hinshewood mechanism[7]

$$\begin{aligned} &\mathrm{CO} + \mathrm{Z} \underset{K_{-1}}{\overset{K_1}{\rightleftharpoons}} \mathrm{ZCO}, \\ &\mathrm{O_2} + 2\mathrm{Z} \xrightarrow{K_2} 2\mathrm{ZO}, \\ &\mathrm{ZCO} + \mathrm{ZO} \xrightarrow{K_3} \mathrm{CO_2} + 2\mathrm{Z}. \end{aligned} \tag{1}$$

The processes of subsurface oxygen formation and its reduction during the reaction are determined as follows:

$$\begin{aligned} &\mathrm{ZO} + \mathrm{Z_V} \xrightarrow{K_4} Z_\mathrm{V}\mathrm{O} + \mathrm{Z}, \\ &\mathrm{ZCO} + \mathrm{Z_VO} \xrightarrow{K_5} \mathrm{CO_2}{+}\mathrm{Z_V}{+}\mathrm{Z}. \end{aligned} \tag{2}$$

A three-variable scaled chemical mechanism can be established, written in the following dimensionless form:

$$\begin{aligned} x' &= K_1(1-x-y) - K_{-1}x - K_3xy, \\ y' &= 2K_2(1-x-y)^2 - K_3xy, \\ z' &= K_4y(1-z) - K_5xz, \end{aligned} \tag{3}$$

where x and y represent the dimensionless concentrations of CO and O absorbed on the surface respectively, and z denotes the dimensionless concentrations of subsurface oxygen. Because all of variables are concentrations, $x, y, z \geqslant 0$, $z \leqslant 1$, $x + y \leqslant 1$. The rate constants of the elementary reactions K_i $(i = 1, -1, 2, 3, 4, 5)$ depend on the partial pressures P_{CO} and $P_{\mathrm{O_2}}$ of oxygen and carbon oxide in the gas phase and on the temperature $T(K)$ as follows:

$$\begin{aligned} &K_1 = 3.6 \times 10^5 P_{\mathrm{CO}}, \quad K_{-1} = 10^{13} \times \exp(-E_1/RT), \\ &K_2 = K_{20} P_{\mathrm{O_2}}, \quad K_3 = 10^{13} \times \exp(-E_3/RT), \end{aligned}$$

where R is the universal gas constant, while E_1 and E_3 are the activation energies of interaction between the adsorbed species . With the assumption that there exist some critical values of the surface coverage with oxygen at which a surface modification occurs, the activation energy E_3, which depends on the concentration y of adsorbed oxygen, can be expressed as

$$E_3 = \begin{cases} E_{31}, & y \leqslant y_c - \delta, \\ E_{32}, & |y - y_c| < \delta, \\ E_{33}, & y \geqslant y_c + \delta, \end{cases} \tag{4}$$

Where E_{31} and E_{33} are constants, while $E_{32} = 25y + 18$ Cal/mol (1 Cal = 1 kcal). The parameters y_c and $0 < \delta \ll 1$ determine the middle and the width of the interval of y values over which E_3 increases (see Fig. 1(a)).

Moreover, due to the oxygen penetration into the subsurface layer, a reconstruction of the metallic surface can occur, changing the adsorption properties of the catalyst. For some critical values of the concentration of subsurface oxygen, K_{20} sharply decreases, which can be described by the following function

$$K_{20} = \begin{cases} K_{21}, & z \leqslant z_c - \delta_1, \\ K_{22}, & |z - z_c| < \delta_1, \\ K_{23}, & z \geqslant z_c + \delta_1, \end{cases} \tag{5}$$

where K_{21} and K_{23} are constants, while $K_{22} = (-39.5 \times z + 24.8) \times 10^4$ $\mathrm{s^{-1}} \cdot \mathrm{Torr^{-1}}$ (1 Torr = 1.33322×10^2 Pa). The parameters z_c and $0 < \delta_1 \ll 1$ determine the middle and the width of the z-interval over which K_{20} decreases (see Fig. 1(b)).

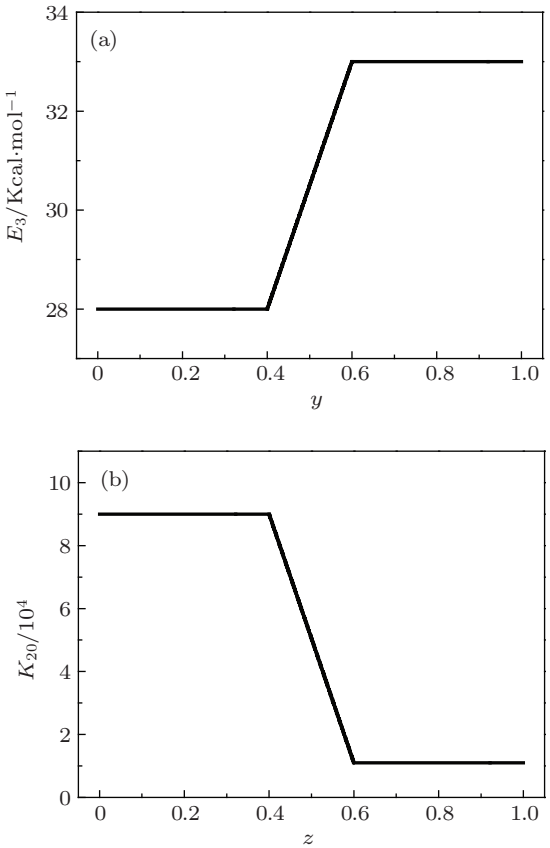


Fig. 1. $y_c = z_c = 0.5$, $\delta = \delta_1 = 0.1$, (a) dependence of E_3 on y, (b) dependence of K_{20} on z.

The parameters fixed in this paper are obtained in the experiment:[7] $T = 500$ K, $P_{\mathrm{O_2}} = 9 \times 10^{-7}$ Torr, $P_{\mathrm{CO}} = 1.1 \times 10^{-7}$ Torr, and the other parameters are listed in Table 1.

Table 1. Values of the activation energies and the rate constants.

$E_1/\mathrm{Cal}\cdot\mathrm{mol}^{-1}$	$E_{31}/\mathrm{Cal}\cdot\mathrm{mol}^{-1}$	$E_{33}/\mathrm{Cal}\cdot\mathrm{mol}^{-1}$	$K_{21}/\mathrm{s}^{-1}\cdot\mathrm{Torr}^{-1}$	$K_{23}/\mathrm{s}^{-1}\cdot\mathrm{Torr}^{-1}$
35	28	33	0.9×10^5	0.11×10^5

Obviously, the processes of adsorption desorption and reactions between adsorbed species are faster than the oxygen penetration and the interaction between subsurface oxygen and adsorbed CO. Therefore, the elementary reaction rate constants K_4 and K_5 are much smaller than K_i, $i=-1,1,2,3$, which implies $K_4 \ll 1$, $K_5 \ll 1$. Here we introduce two parameters ε and α, with $\varepsilon = K_5$, $\alpha = K_4/K_5$ for convenience and fix $\varepsilon = 0.00003$, $A = 4.645$.

Furthermore, a small perturbation may exist which affects the change of the dimensionless concentration of CO absorbed on the surface. Here we assume that the perturbation varies periodically, which leads to the modified model expressed in the form

$$x' = K_1(1-x-y) - K_{-1}x - K_3xy + a\cos\omega t, \quad (6a)$$

$$y' = 2K_2(1-x-y)^2 - K_3xy, \quad (6b)$$

$$z' = K_4y(1-z) - K_5xz = \varepsilon(\alpha y(1-z) - xz), \quad (6c)$$

where a and ω measure the amplitude and the frequency of the perturbation, respectively.

The elementary reaction rate in the subsurface layer is much slower than that on the surface, which yields the different timescales involved in the system, implying that variables x and y change on a faster timescale than variable z in several reaction steps. Therefore, the full system (6) can be divided into slow and fast subsystems. The slow subsystem (SS), is given by Eq. (6c), while the fast subsystem (FS) by Eqs. (6a) and(6b).

The system with multiple timescales often behaves in periodic bursting phenomena characterized by a combination of relatively large amplitude and nearly harmonic small amplitude oscillation. We say the reaction is in a quiescent state (QS) if all the variables are at rest or exhibit small amplitude oscillations. It can fire spikes (SP) periodically when a large amplitude limit cycle attractor exists. The quiescent state and SP are mainly determined by the slow and fast systems.

To reveal the bifurcation mechanism of bursting behaviors, a quasi-steady-state will be used to reduce the dimension of the vector field, i.e., consider the slow variable z as the bifurcation parameter of the FS. Periodic bursting phenomena occur when the reaction alternates between a QS and SP, in which two important bifurcations can be observed: bifurcation of a QS leading to repetitive SP and bifurcation of SP to a QS.

3. Bursting behaviors as well as bifurcation mechanism

It is noted that the value of perturbation $p = a\cos\omega t$ may change between $p_1 = a$ and $p_2 = -a$. By taking the slow variable z as a bifurcation parameter, two patterns of bifurcation details can be obtained, which correspond to the extreme cases with $p = p_{1,2}$, respectively. Because the perturbation is confined to the two cases, the mechanism of slow–fast behaviors of the full system can be explained by employing these two bifurcation patterns, combining with the trajectory of the full system. The method, called enveloping slow–fast analysis, will be used to investigate the dynamic evolution of the full system in the following.

3.1. Fold/Fold/Hopf bursting

Firstly, the oscillation of the system is taken into consideration with a relatively large perturbation frequency, which implies that the change of the values of the perturbation varies critically. For the fixed parameters $k_1 = 0.0396$, $a = 0.0014$, $\omega = 0.095$, a periodic burster can be observed, the phase portrait of which is shown in Fig. 2(a), while the projection on the y–z plane is presented in Fig. 2(b). The direction of the trajectory on the y–z phase is counterclockwise, which can be demonstrated by using the time history plotted in Figs. 2(c) and (2d).

By employing the enveloping slow–fast analysis, the two equilibrium curves E_{q_1} and E_{q_2} for $p = \pm 0.0014$ of the fast subsystem are presented in Fig. 3(a), with the variation of the slow variable z, where L_{11}, L_{12}, and H_1 are the critical points for the fold bifurcation and Andronv–Hopf bifurcation of the fast-subsystem, respectively, for $p = 0.0014$. While L_{21}, L_{22}, and H_2 are the critical points for the fold bifurcation and Andronv–Hopf bifurcation, respectively, for $p = -0.0014$. Note that the dashed branches represent unstable equilibria, while the solid is stable equilibria.

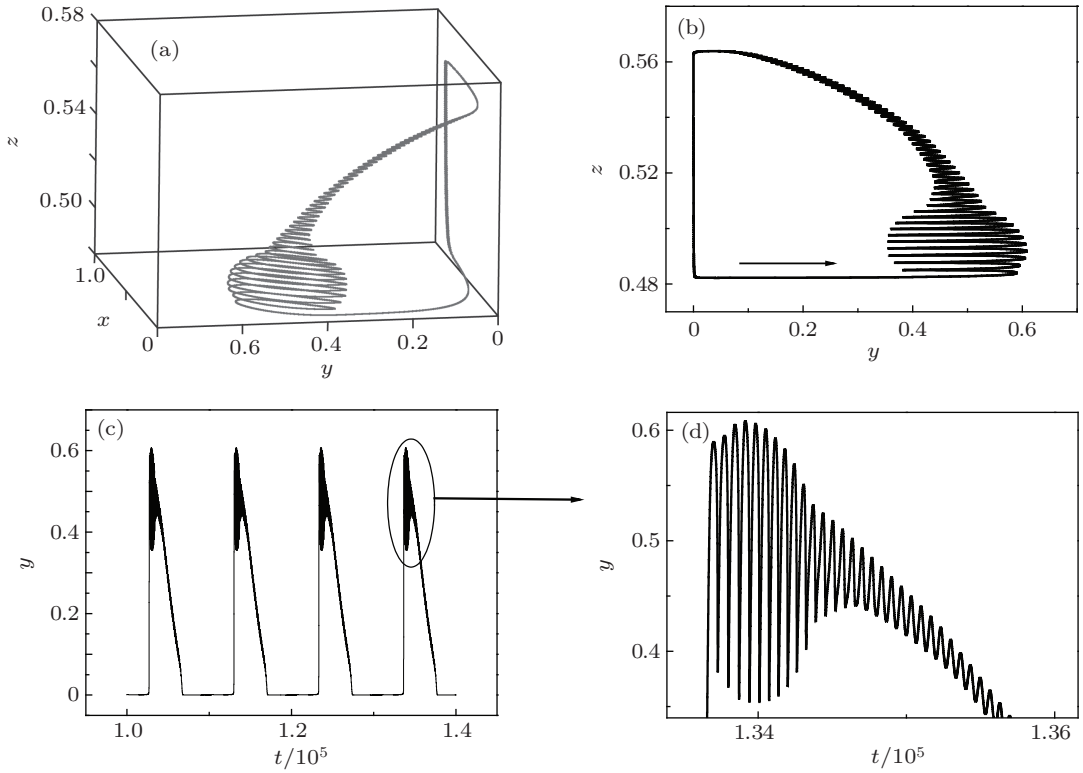


Fig. 2. $K_1 = 0.0396$, $a = 0.0014$, $\omega = 0.095$. (a) Three-dimensional phrase portrait, (b) the projection of transformed phase portrait onto y–z plan, (c) time history, and (d) the local enlargement for panel (c).

To explore the bifurcation mechanism of the burster, we overlap the bifurcation diagram as well as the phase portrait on the y–z plane, as shown in Fig. 3(b). It can be checked that the whole trajectory of the periodic burster is almost confined to the two equilibrium curves E_{q_1} and E_{q_2} except the large-amplitude oscillations around H_1 and H_2. The trajectory, starting from the point A with y approximated at 0.36, moves with large-amplitude oscillations, which can be called repetitive SP, until the point B around H_2. Hopf bifurcation associated with the fast subsystem occurs, leading the trajectory to small-amplitude oscillations, which implies that the system changes from SP to a QS via Hopf bifurcation. The amplitudes of the oscillations reduce to zero when the trajectory moves near the point C, at which fold bifurcation takes place. A jumping phenomenon can be observed, which leads the trajectory to steadily move from point C to point D, at which another fold bifurcation occurs, resulting in the jumping phenomenon, corresponding to the quick movement of the trajectory from point D to point A. The trajectory then completes the whole periodic bursting, called Fold/Fold/Hopf bursting.

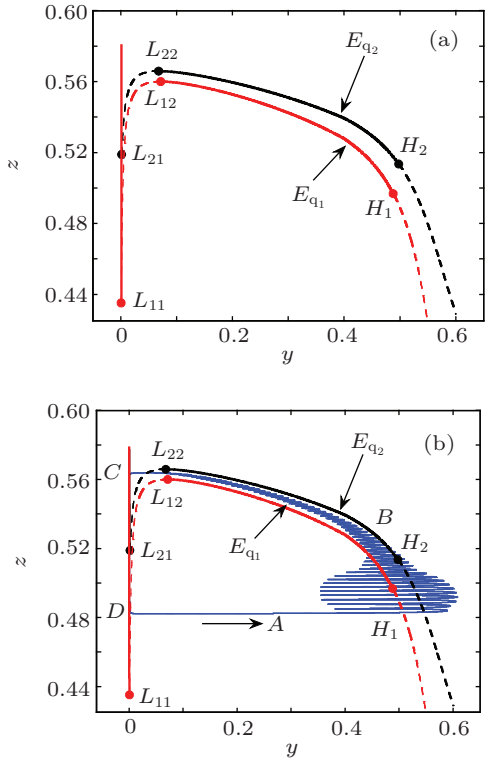


Fig. 3. (colour online) $K_1 = 0.0396$, $a = 0.0014$, $\omega = 0.095$. (a) The bifurcation diagram with respect to z for $p_1 = 0.0014$ in E_{q_1} and $p_2 = -0.0014$ in E_{q_2}, (b) the overlay of the bifurcation diagram with the projection of transformed phase portrait onto y–z plan.

Here we would like to point out two phenomena during the periodic bursting of the system. Firstly, after the point B corresponding to Hopf bifurcation of the fast-subsystem, the trajectory related to the small-amplitude oscillation is full confined to the two equilibrium curves E_{q_1} and E_{q_2}. Since the value of the periodic perturbation varies from p_1 to p_2, while both the equilibrium states from L_{12} to H_1 and from L_{22} to H_2 are stable, therefore, the trajectory may alternates between the two approaching trends to E_{q_1} and E_{q_2}, which results in the small-amplitude oscillations of the trajectory. Secondly, the value of z related to the fold bifurcation point C can be observed between the values of z related to two fold bifurcation points L_{12} and L_{22}, of the fast subsystem, while D between L_{11} and L_{21}, which implies that the transition points of the trajectory confine to the bifurcations of the fast subsystem.

Further investigation reveals that three frequencies are involved in the periodic bursting phenomenon. The period of the burster can be determined by the natural frequency ω_n approximated at 0.000613, while the small-amplitude oscillations from point B to point C vibrate according to the frequency of the perturbation $\omega = 0.095$. Furthermore, the frequencies related to H_1 and H_2 can be computed approximated at 0.08376 and 0.1265, which results in the frequency of large-amplitude oscillation from point A to point B at $\omega_s \approx 0.0915$.

3.2. Fold/Fold bursting

If the parameters change to $k_1 = 0.0278$, $a = 0.002$, $\omega = 0.02$, Hopf bifurcation points H_1 and H_2 of the fast-subsystem separate from the trajectory of the full system, which leads to another type of bursting phenomenon case (see Fig. 4).

The trajectory, starting from point A with oscillations moving to point C, at which fold bifurcation occurs, the jumping phenomenon can be observed, which leads the trajectory to the movement from point C to point D, while another fold bifurcation takes place, resulting in the jumping of the trajectory from point D to point A. Therefore the periodic solution can be called Fold/Fold bursting.

Note that no Hopf bifurcation can be observed related to the trajectory, which implies only two frequencies are involved in the oscillation, i.e., the natural frequency and the perturbation frequency.

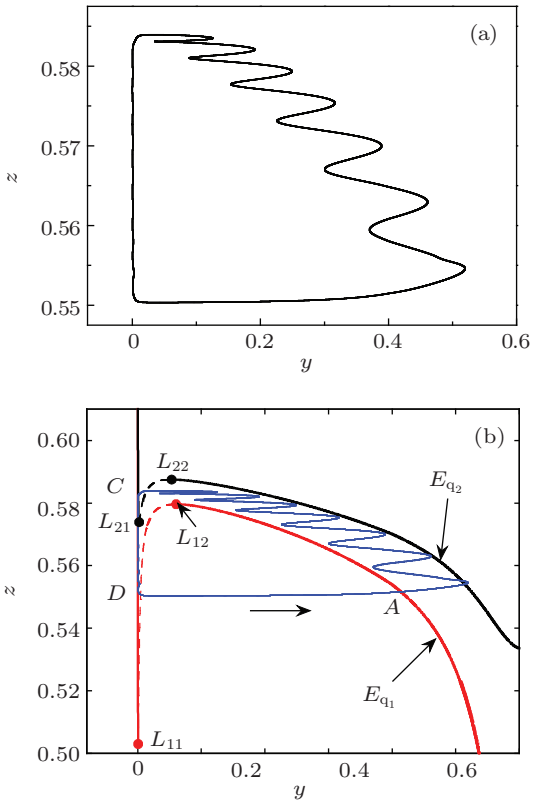


Fig. 4. (colour online) $K_1 = 0.0278$, $a = 0.002$, $\omega = 0.02$. (a) Projection of the phase portrait onto the y–z plan; (b) the overlay of the bifurcation diagram for $p_1 = 0.002$ in E_{q_1} and $p_2 = -0.002$ in E_{q_2} with the projection of then transformed phase portrait onto the y–z plan.

3.3. Bursting mechanism with low perturbation frequency

Now we decrease the frequency of the periodic perturbation to 0.0095 to investigate the periodic bursting of the full system. The overlay of the bifurcation details of the fast subsystem and the phase portraits with different values of the amplitude of periodic perturbation is shown in Fig. 5. Note that from the three cases, Hopf bifurcation is involved in the periodic bursting only for $a = 0.001$. Bifurcation mechanisms related to Fold/Fold/Hopf bursting in Fig. 5(a) and Fold/Fold bursting in Figs. 5(b) and 5(c) are similar to those described above.

The purpose of Fig. 5 is to describe the frequencies involved in the bursters more clearly. It can be checked that only two frequencies, i.e., the natural frequency and the perturbation frequency, are involved in the Fold/Fold bursters in Figs. 5(b) and 5(c). However for the Fold/Fold/Hopf bursting in Fig. 5(a), computation reveals that the frequencies related to H_1 and H_2 are $\omega_{H_1} \approx 0.124$, $\omega_{H_2} \approx 0.153$, which lead to the frequency of the repetitive spiking from point

A to point B, approximated at $\omega_s = 0.141$. While the small-amplitude oscillations vibrate according to the frequency of the perturbation at $\omega = 0.0095$, and the period of the buster is determined by the natural frequency $\omega_n = 0.0007288$.

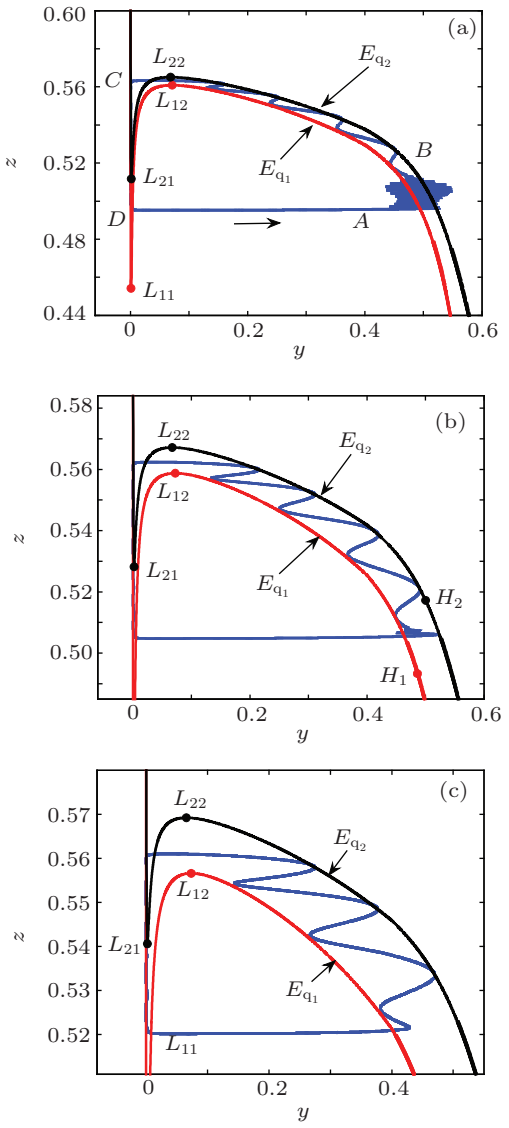


Fig. 5. (colour online) The overlay of the bifurcation diagrams with the projection of transformed phase portraits onto the y–z plan for $K_1 = 0.0396$, $\omega = 0.0095$. (a) Fold/Fold/Hopf bursting for $p_1 = 0.001$ in E_{q_1} and E_{q_2}, (b) Fold/Fold bursting for $p_1 = 0.002$ in E_{q_1} and $p_2 = -0.002$ in E_{q_2}, (c) Fold/Fold bursting for $p_1 = 0.003$ in E_{q_1} and $p_2 = -0.003$ in E_{q_2}.

Here we would like to point out that when the frequency related to the periodic perturbation is much less than the two frequencies associated with the Hopf bifurcations of E_{q_1} and E_{q_2}, for the Fold/Fold/Hopf bursting, obvious separation between the small-amplitude oscillations and the large-amplitude oscillations can be observed. Furthermore, for the Fold/Fold bursting, because of the small frequency of the perturbation, the oscillating times may be greatly reduced compared to the case related to the bursting with a relatively large frequency of periodic perturbation.

4. Conclusion

Based on the traditional slow–fast analysis for autonomous nonlinear systems with multiple time scales, the enveloping slow–fast analysis method is developed to explore the dynamical behaviors of the kinetic model of CO oxidation on the platinum group metals with periodic perturbation. Two typical bursting phenomena have been presented, which can be called Fold/Fold/Hopf bursting and Fold/Fold bursting, respectively, according to the bifurcation forms between the QS and the repetitive SPs. It is found that when the Hopf bifurcation occurs before the alternation between small-amplitude oscillation and the steady state, large-amplitude oscillations can be observed for the bursting, and a new frequency associated with the Hopf bifurcation may describe the approximation of the frequency of the spiking corresponding to the large-amplitude oscillations. On the other hand, if the Hopf bifurcation takes place after the alternation, only fold bifurcation is involved in the bursting, which results in no large-amplitude oscillations.

Furthermore, when the frequency of the perturbation is much less than the frequencies associated with the Hopf bifurcation corresponding to two equilibrium curves, respectively, for the Fold/Fold/Hopf bursting, an obvious separation between the small-amplitude oscillations and the large-amplitude oscillations can be observed, while for the Fold/Fold bursting, the times of the small-amplitude oscillations may be greatly reduced, compared with the case with a relatively large frequency of periodic perturbation. It can also be found that the natural frequency determines the period of the bursting, the perturbation frequency describes the frequency of the small-amplitude oscillations, and the frequencies associated with the Hopf bifurcation of the fast subsystem, if they take place, define the approximation of the frequency of the large-amplitude oscillations.

References

[1] Neugebauer J, Zywietz T, Scheffler M, *et al.* 2003 *Phys. Rev, Lett.* **90** 056101

[2] Davis M J and Klippenstein S J 2002 *J. Phys. Chem.* **106** 5860

[3] Rinzel J and Lee Y S 1987 *J. Math. Biol.* **25** 653

[4] Fujimoto F and Kaneko K 2003 *Physica* D **180** 1

[5] Conforto F, Groppi M and Jannelli A 2008 *Appl. Math. Comput.* **206** 892

[6] He J H and Xu F 2009 *Comput. Math. Appl.* **58** 2431

[7] Lashina E A, Chumakova N A, Chumakov G A and Boronin A I 2009 *Chem. Eng. J.* **154** 82

[8] Chumakov G A, Slinko M M, Belyaev V D and Slinko M G 1977 *Dokl. Akad. Nauk. USSR* **234** 399

[9] Slinko M M and Jeager N I 1994 *Stud. Surf. Sci. Catal.* **86** 415

[10] Eiswirth M and Krischer K 1988 *Surf. Sci.* **202** 565

[11] Boronin A I and Nizovskii A I 1989 *Institute of Catalysis, Novosibirsk* 39

[12] Elokhin V I and Boronin, A I 1989 *Institute of Catalysis, Novosibirsk* 62

[13] Latkin E I, Elokhin V I and Gorodetskii V V 2001 *J. Mol. Catal.* A: *Chem.* **166** 23

[14] Yang Z Q and Lu Q S 2008 *J. Biol. Sys.* **16** 33

[15] Han X and Bi Q 2009 *Acta Phys. Sin.* **58** 4408 (in Chinese)

[16] Li X and Bi Q 2012 *Acta Phys. Sin.* **61** 020504 (in Chinese)

[17] Bi Q 2010 *Sci. Chin.*: *Tech. Sci.* **53** 748

[18] Rinzel J 1985 *Ordinary and Partial Differential Equations* (Berlin: Springer-Verlag) p. 304